Supporting Information

A Versatile Luminescent Metal-Organic Framework for Selective Detection of Fe(III) Cations and Cr(VI) Anions

Han Fang,[a] Jia-Peng Han,[a] Bo Zhang,[a] Deng-Bo Liu,[a] Xing-Wang Li,[a] Jing-Yu Li,[a] Yutong He,[,b] and Mei-Hui Yu*[,a]*

[a] *School of Materials Science and Engineering, National Institute for Advanced Materials, Tianjin Key Laboratory of Metal and Molecule-Based Material Chemistry, Nankai University, Tianjin 300350, China*

[b] *School of Chemical Engineering and Technology, Tianjin University, Tianjin 300072, China*

* Corresponding author.

E-mail: heyt@tju.edu.cn (Y. He);

mh@nankai.edu.cn (M.-H. Yu)

Table S1. Crystallographic data and structure refinement of **NKM-103**.

Identification code	**NKM-103**
Empirical formula	$C_{43}H_{24}Cd_2F_4N_6O_8$
Formula weight	1053.48
Temperature/ K	300.48(10)
Crystal system	Monoclinic
Space group	*C*2/*c*
a/Å	26.9074(4)
b/Å	17.1592(3)
c/Å	27.3590(4)
a/°	90
b/°	96.1830(10)
g/°	90
Unit cell volume/ $Å^3$	12558.4(3)
Z	8
Density (calculated)	1.114 g/cm^3
F(000)	4160.0
Radiation	CuKα (λ = 1.54184)
2θ range for data collection/°	6.12 to 154.328
Independent reflections	13062 [R(int) = 0.0587]
Data/restraints/parameters	13062/0/568
Goodness-of-fit on F^2	1.089
Final R indexes [I>=2σ (I)]	R_1 = 0.0393, wR_2 = 0.1106
Final R indexes [all data]	R_1 = 0.0425, wR_2 = 0.1132

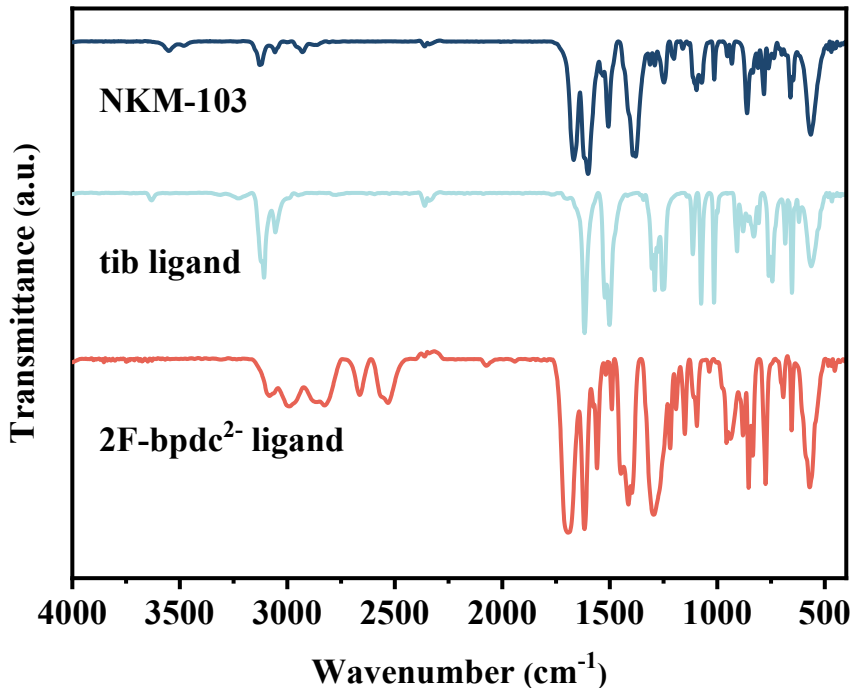

Figure S1. Fourier transform infrared spectra of the ligands and **NKM-103**.

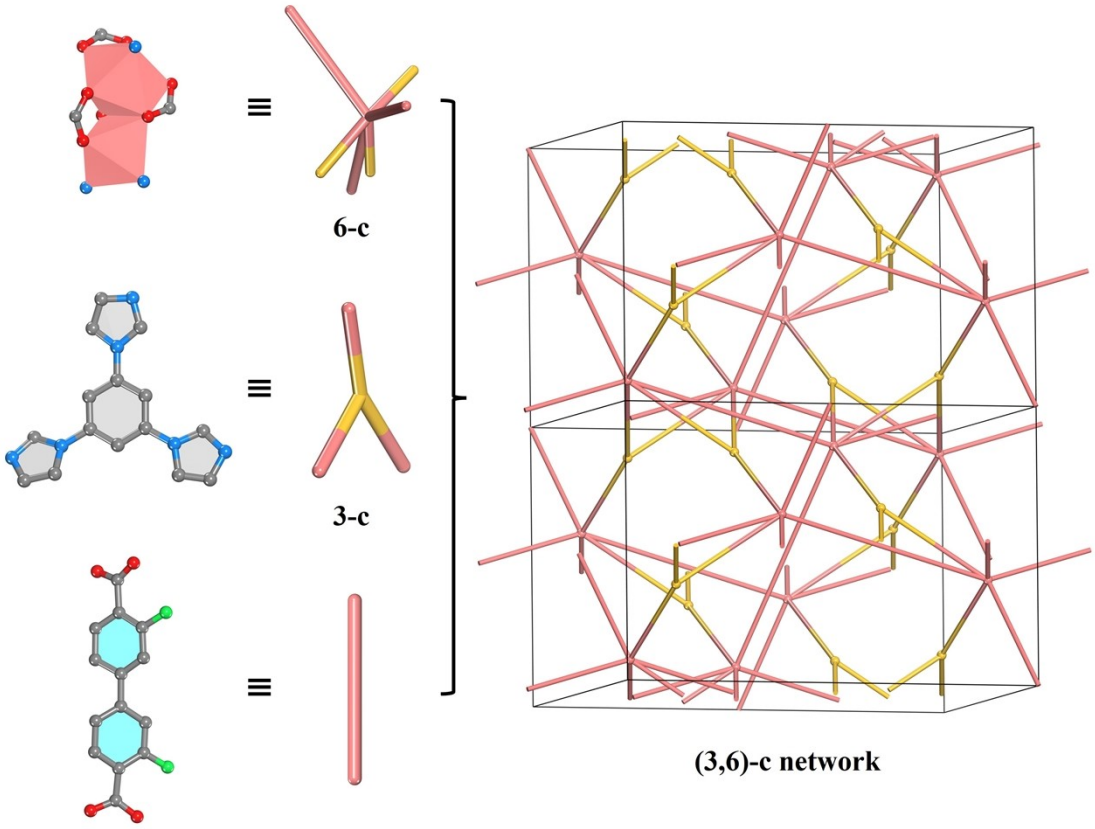

Figure S2. The schematic representative of the topology analysis for **NKM-103**.

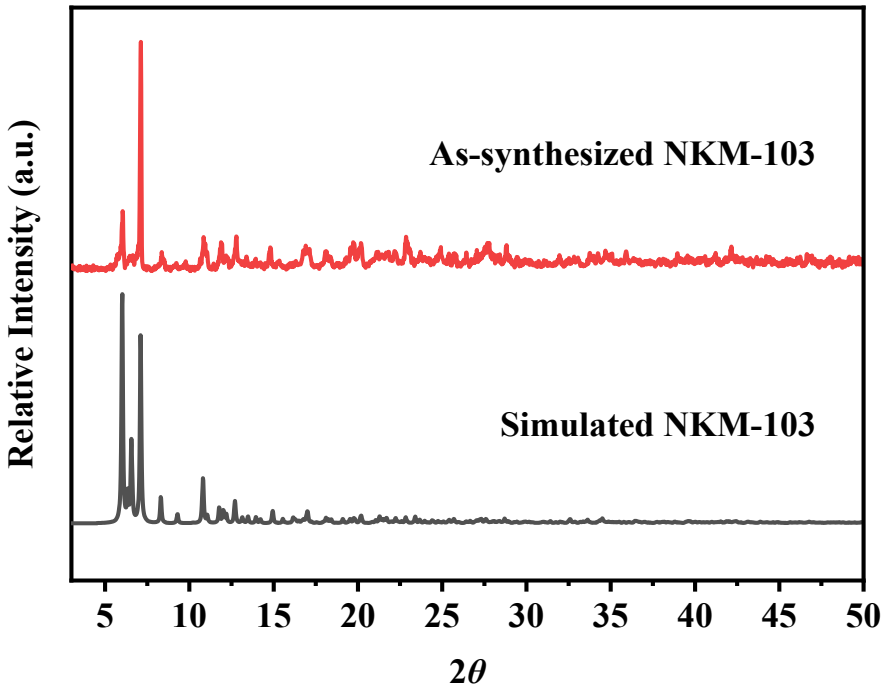

Figure S3. PXRD patterns of **NKM-103** and the simulated one based on the crystal X-ray diffraction result.

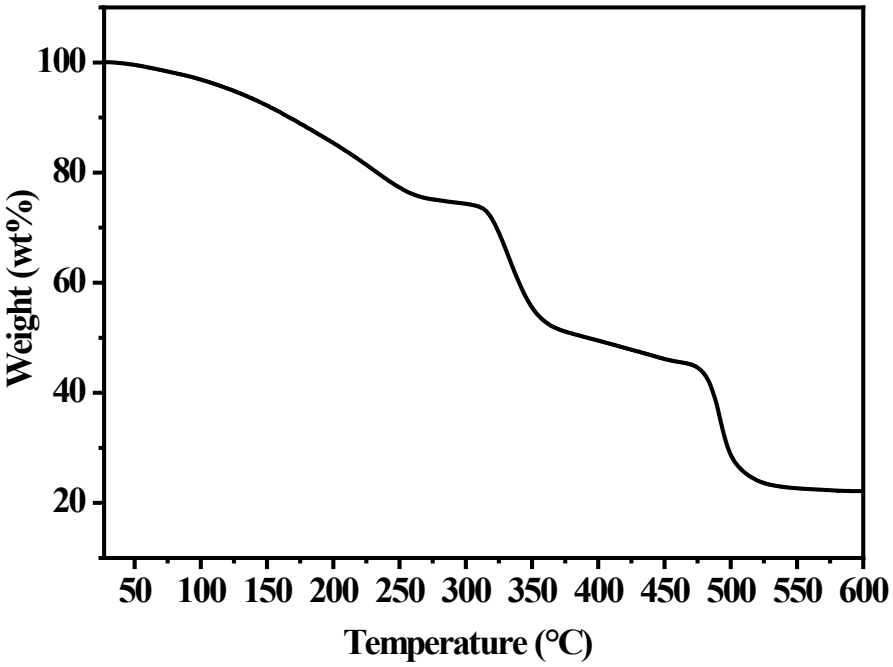

Figure S4. TGA curve of **NKM-103**.

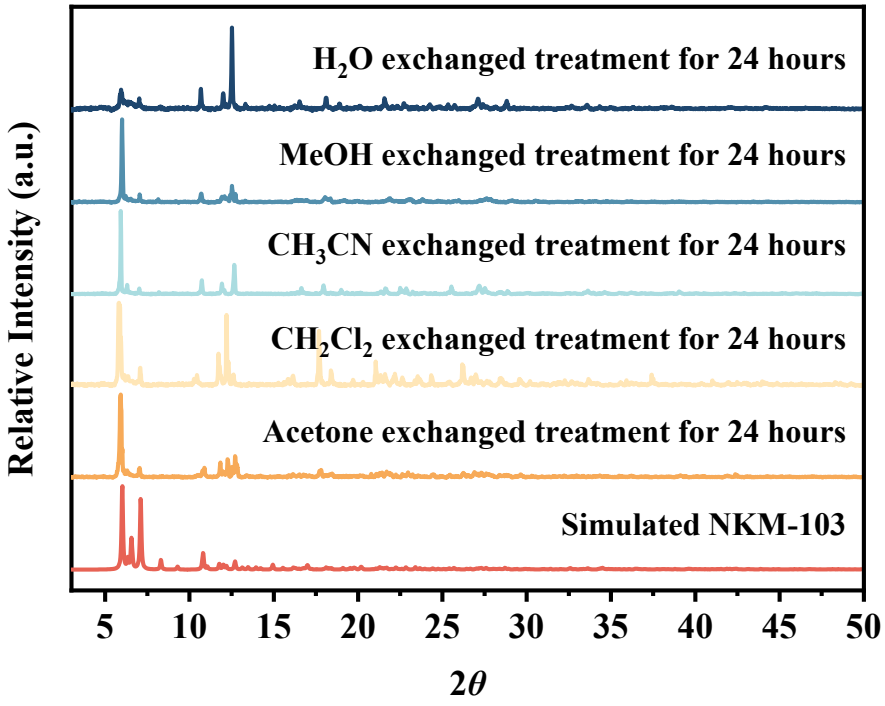

Figure S5. PXRD patterns of **NKM-103** after different solvent exchanged treatment for 24 hours.

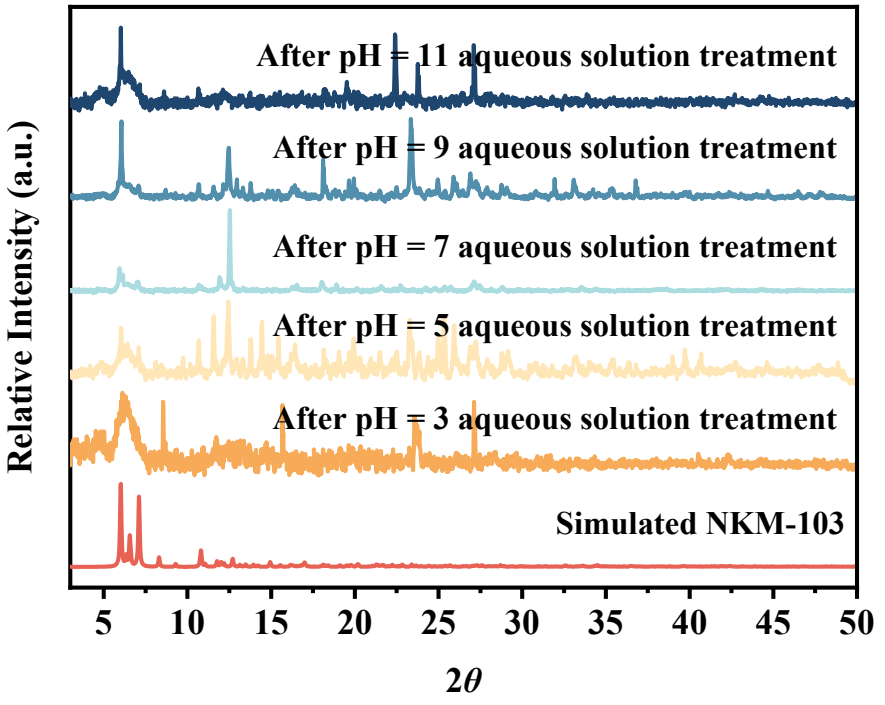

Figure S6. PXRD patterns of **NKM-103** after different pH (3-11) aqueous solvent treatment for

24 hours.

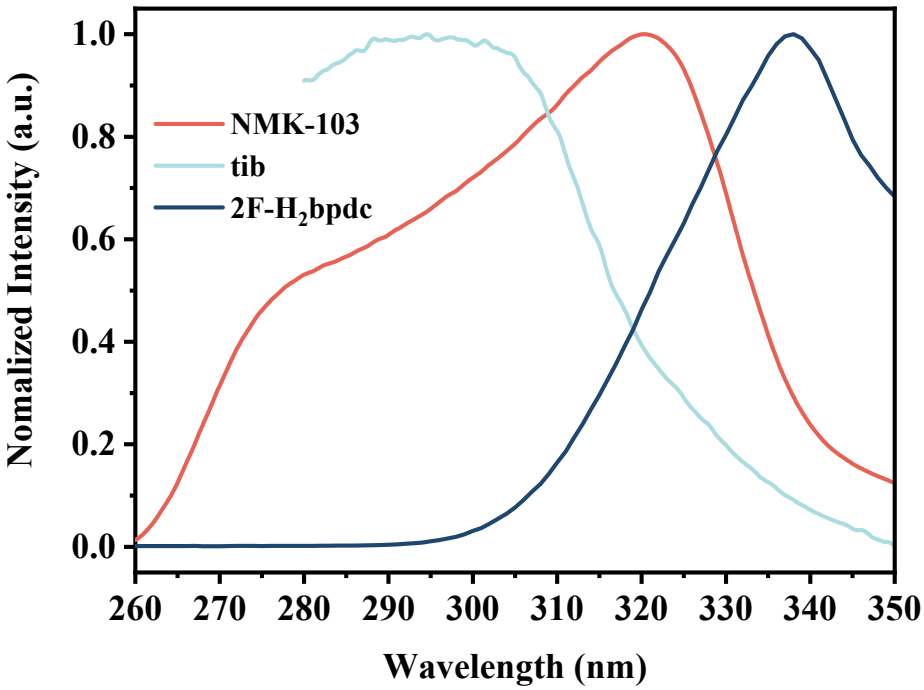

Figure S7. Normalized solid-state excitation spectra of **NKM-103**, tib and 2F-H_2bpdc.

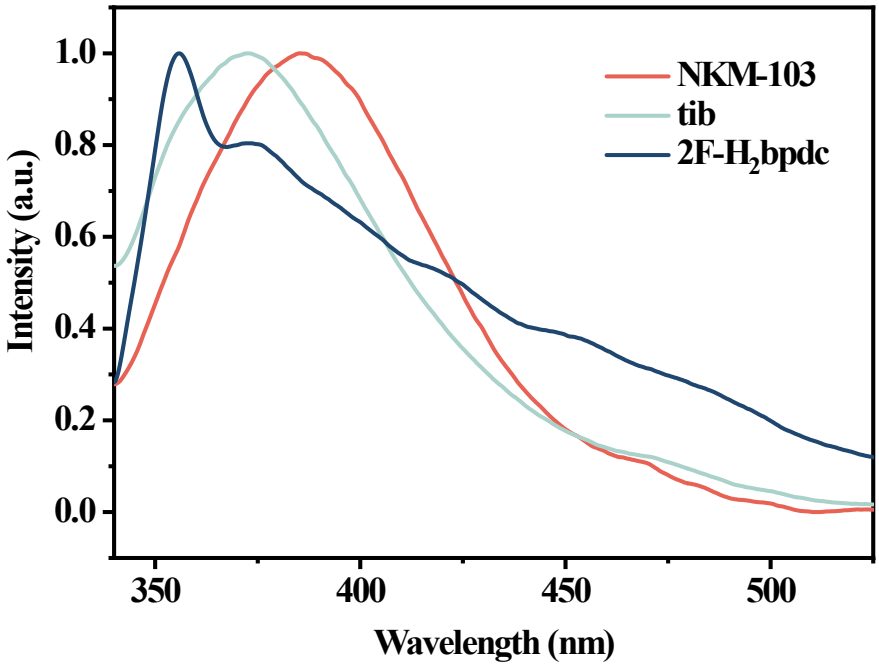

Figure S8. Normalized solid-state emission spectra of **NKM-103**, tib and 2F-H_2bpdc.

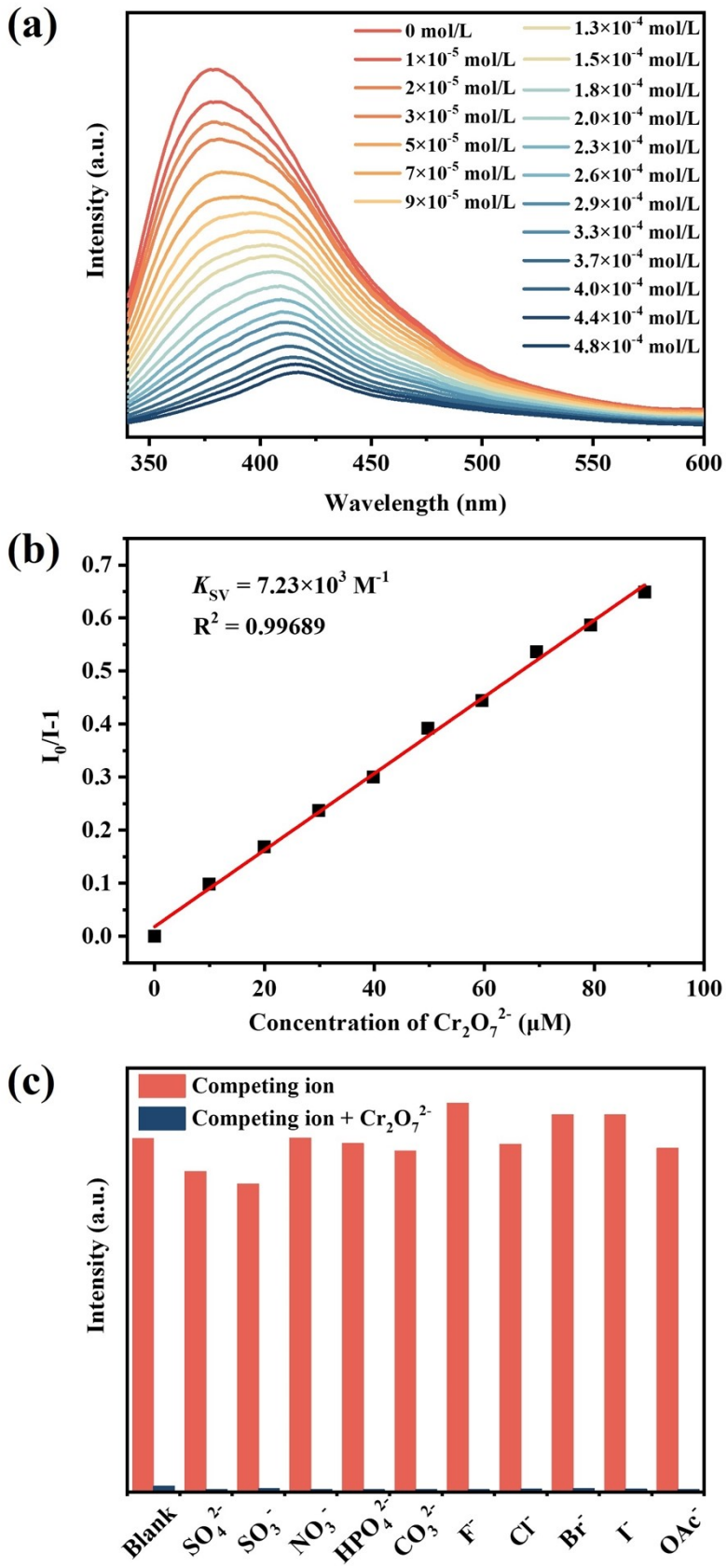

Figure S9. (a) Emission spectra of the **NKM-103** at different CrO_4^{2-} concentrations (b) The Stern-Volmer curve $I_0/I-1$ vs. the concentration of CrO_4^{2-}; (c) Anti-jamming tests of **NKM-103** with the

addition of coexisting ions and CrO_4^{2-}.

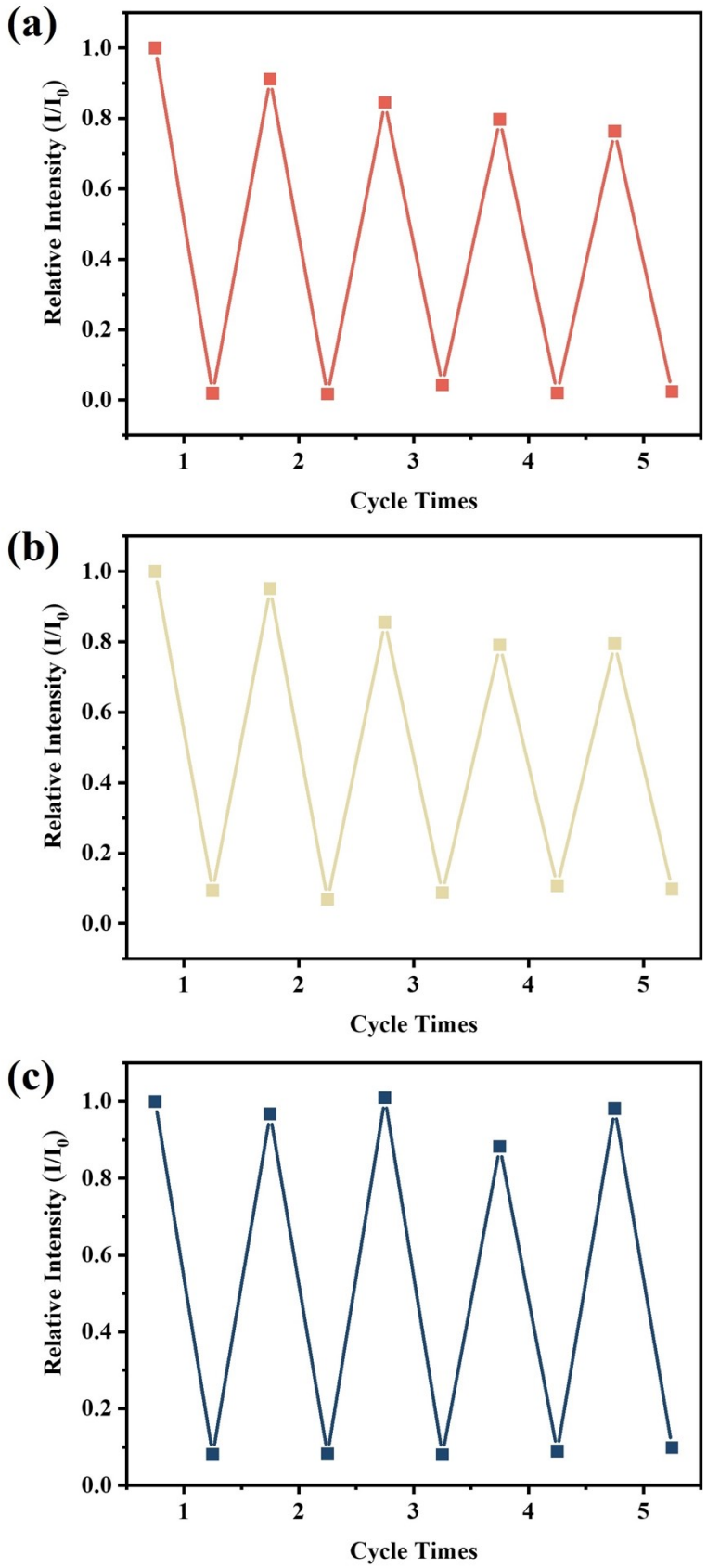

Figure S10. The relative fluorescence intensity in the cyclic tests of **NKM-103** for sensing (a) Fe^{3+},

(b) CrO_4^{2-} and (c) $Cr_2O_7^{2-}$.

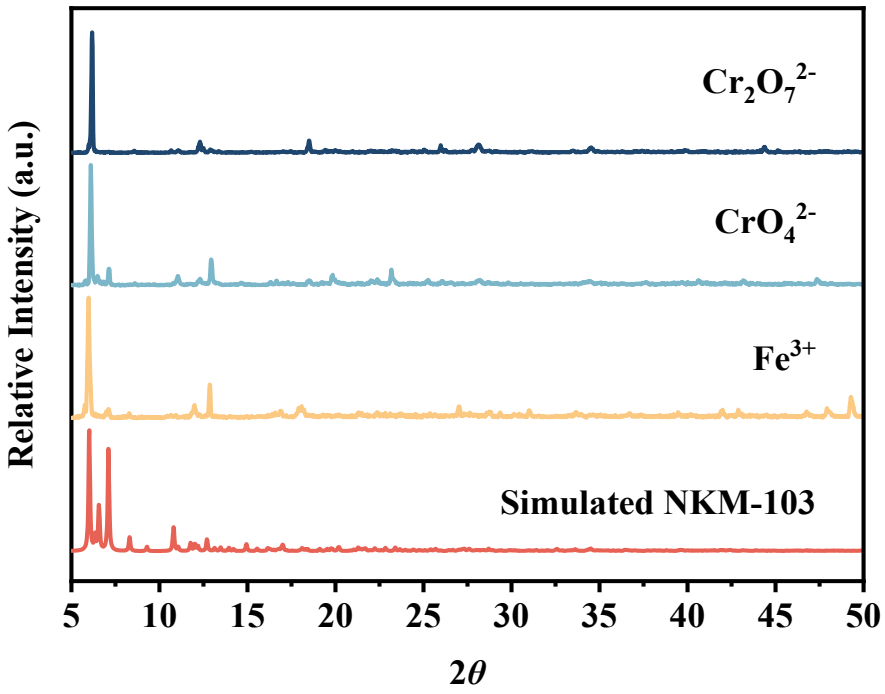

Figure S11. PXRD pattern of **NKM-103** after five cyclic tests of Fe^{3+}, CrO_4^{2-} and $Cr_2O_7^{2-}$.

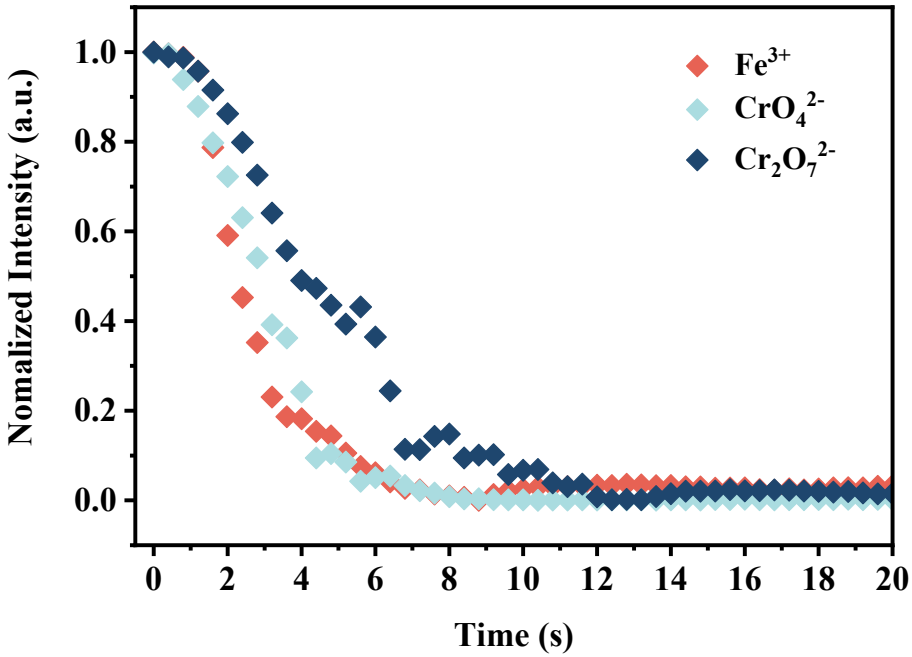

Figure S12. Time-resolved fluorescence decay curves of **NKM-103** in the presence of Fe^{3+}, CrO_4^{2-}

and Cr_2O7^{2-}, respectively.

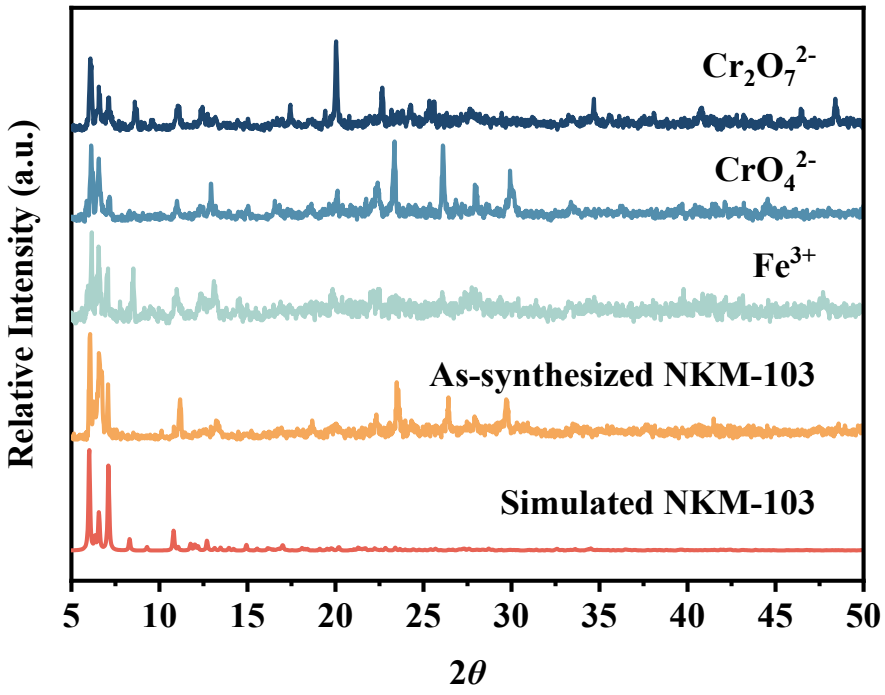

Figure S13. PXRD patterns of **NKM-103** after immersion in the solutions containing Fe^{3+}, CrO_4^{2-} and $Cr_2O_7^{2-}$ for 10 h, with reference to the simulation result.

Table S2. Comparison of luminescent materials for Fe^{3+}.

luminescent materials	K_{sv} (M^{-1})	detection limit (ppm)	Ref.
NKM-103	6.67×10^4	7.06	This work
$\{[Cd(L)(SDBA)(H_2O)]\cdot 0.5H_2O\}_n$	3.59×10^4	1.16	1
Cd-MOF	1.2×10^4	28.71	2
$\{[Zn(L)(dcdps)]\}_n$	7.004×10^3	1.01	3
$\{Zn(L)(bdc)\}_n$	9.066×10^3	7.21	3
$\{[Cd(L)(oba)]\cdot 0.5DMF\}_n$	4.984×10^3	18.69	3
$\{[Cd(L)(bdc)\cdot 2H_2O]\cdot 2DMF\}_n$	6.387×10^3	10.32	3
PAF-5CF	1.187×10^5	6.16	4
$[(CH_3)_2NH_2][Ca(Me_2tcpbH)(H_2O)$	1.18×10^5	3.38	5

Table S3. Comparison of luminescent materials for CrO_4^{2-}.

luminescent materials	K_{sv} (M^{-1})	detection limit (ppm)	Ref.
NKM-103	5.25×10^3	79.15	This work
$[Zn_2(ttz)H_2O]_n$	2.35×10^3	23.2	6
$[Zn(btz)]_n$	3.19×10^3	11.6	6

Cd-MOF	2.4×10^3	209.7	2
$[Zn(IPA)(L)]_n$	1.00×10^3	21.3	7
$[Cd(IPA)(L)]_n$	1.30×10^3	2.92	7

Table S4. Comparison of luminescent materials for $Cr_2O_7^{2-}$.

luminescent materials	K_{sv} (M^{-1})	detection limit (ppm)	Ref.
NKM-103	7.23×10^3	212.47	This work
Cd-MOF	1.4×10^4	40.21	2
$\{[Zn_2(Hbtc)_2(BTD\text{-}bpy)(MeOH)_2]\cdot MeOH\}_n$	6.12×10^3	514.53	8
$\{[Zn_2(1,4\text{-}ndc)_2(BTD\text{-}bpy)]\cdot 0.5MeOH\cdot H_2O\}_n$	8.94×10^3	162.14	8
$Zn_2(tpeb)(bpdc)_2$	1.12×10^4	224.84	9
$[Zn(L)_2]\cdot 2DMF$	1.25×10^4	313.48	10
$[Zn_2(ttz)H_2O]_n$	2.19×10^3	43.2	6
$[Zn(btz)]_n$	4.23×10^3	4.32	6
$\{[Cd(L)(SDBA)(H_2O)]\cdot 0.5H_2O\}_n$	4.97×10^3	105	11

References

[1] S.-G. Chen, Z.-Z. Shi, L. Qin, H.-L. Jia and H.-G. Zheng, *Cryst. Growth Des.,* 2017, **17**, 67-72.

[2] W. Cai, Y.-T. Yan, X.-D. Fan, H. Zhang, J.-L. Lu, Y.-L. Wu, J. Liu, W.-Y. Zhang and Y.-Y. Wang, *J. Mol. Struct.,* 2024, **1302**, 137528.

[3] F.-Y. Ge, G.-H. Sun, L. Meng, S.-S. Ren and H.-G. Zheng, *Cryst. Growth Des.,* 2020, **20**, 1898-1904.

[4] T. Ma, X. Zhao, Y. Matsuo, J. Song, R. Zhao, M. Faheem, M. Chen, Y. Zhang, Y. Tian and G. Zhu, *J. Mater. Chem. C.,* 2019, **7**, 2327-2332.

[5] Z.-F. Wu, Z.-H. Fu, E. Velasco, K. Xing, H. Wang, G.-D. Zou, X.-Y. Huang and J. Li, *J. Mater. Chem. C,* 2020, **8**, 16784-16789.

[6] C.-S. Cao, H.-C. Hu, H. Xu, W.-Z. Qiao and B. Zhao, *Cryst. Eng. Comm.,* 2016, **18**, 4445-4451.

[7] P. Bhavesh, R. Yadagiri, K. B. Kamal, L. Ridhdhi, S. Eringathodi, *Inorg. Chem.,* 2017, **56**, 2627-2638.

[8] Q. J. Jiang, J. Y. Lin, Z. J. Hu, V. K. S. Hsiao, M. Y. Chung and J. Y. Wu, *Cryst. Growth Des.,* 2021, **21**, 2056-2067.

[9] B. B. Rath and J. J. Vittal, *Inorg. Chem.,* 2020, **59**, 8818-8826.

[10] B. Li, Q. Q. Yan and G. P. Yong, *J. Mater. Chem. C,* 2020, **8**, 11786-11795.

[11] S. Chen, Z. Shi, L. Qin, H. Jia and H. Zheng, *Cryst. Growth Des.,* 2016, **17**, 67-72.